Journal of Hard Tissue Biology 14[1] (2005 p32-37)

CODEN-JHTBFF, ISSN 1341-7649

Original

Identification of Reduced Fibronectin 1 Gene Expression in Osteoblasts following Hydrogen Peroxide Treatment using Subtractive Gene Cloning

Susumu Hamajima[1)], Toshinori Sato [2)], Yoko-Otsuka Tanaka [2,3)], Chia-Hua Yang [1)], Nobuyuki Watanabe [1)], Junichi Mega [2,3)], Toshiro Sakae [3,4)] and Yoshimitsu Abiko [1, 3)]

1) Department of Biochemistry and Molecular Biology, Nihon University School of Dentistry at Matsudo, Chiba 271-8587, Japan.
2) Department of Dentistry for the Disabled, Nihon University School of Dentistry at Matsudo, Chiba 271-8587, Japan
3) Research Institute of Oral Sciences, Nihon University School of Dentistry at Matsudo, Chiba 271-8587, Japan.
4) Department of Histology, Cytology and Developmental Anatomy, Nihon University School of Dentistry at Matsudo, Chiba 271-8587, Japan
(Accepted for publication, February 15, 2005)

Abstract: Bone formation steadily declines with age resulting in a significant loss of bone mass, while reactive oxygen species (ROS) are thought to be major contributors to the aging process. In the present study, we attempted to identify which gene had an altered transcription level when osteoblasts were treated with ROS, H_2O_2, using a subtraction gene cloning technique. A gene clone was obtained from cDNA of cells from the osteoblastic cell line MC3T3-E1 after subtraction of the cDNA of H_2O_2-treated cells and designated as MC-ROS-7. To confirm the gene product, the DNA sequence of MC-ROS-7 was determined and homology was assessed using a nucleotide-nucleotide BLAST (BLASTN) search of the NCBI database, which revealed a 99.7% homology with fibronectin 1 (FN) gene. A significant lower level of FN mRNA was found in H_2O_2-treated cells when compared to that in non-treated cells using endpoint RT-PCR and real-time PCR assays. Our results suggest that a reduction of FN gene expression by ROS is involved in the decline of bone formation in osteoblasts during the ageing process.

Key words: Ageing, Fibronectin, Gene Expression, Osteoblasts

Introduction

Bone remodeling requires a delicate balance between bone formation and bone resorption, in which bone-forming osteoblasts and bone-resorbing osteoclasts play central roles[1)]. It is well known that bone formation steadily declines with age, resulting in a significant loss of bone mass, and may be due to a decrease in osteoblast proliferating precursors or the number of pre-osteoblasts that differentiate, or possibly decreased synthesis and secretion of essential bone matrix proteins[2)]. However, the nature of the mechanisms that underlie the aging process and their effects on bone metabolism are not well understood. A currently popular hypothesis states that reactive oxygen species (ROS), produced during normal cellular metabolism, are major contributors to the aging process[3)].

ROS include superoxides anions, hydroxyl radicals, and H_2O_2, which can cause severe damage to DNA, protein, and lipids. High levels of oxidants produced during normal cellular metabolism or from environmental stimuli disturb the normal redox balance and shift cells into a state of oxidative stress[4)]. Recent evidence has shown that ROS may be involved in the pathogenesis of bone loss-related diseases, a marked decrease in plasma antioxidants was found in aged osteoporotic women[5)]. Osteoporosis was noted in 2 different mouse models of premature aging associated with oxidative damage, in which osteopenia was speculated to be the consequence of oxidative damage[6, 7)]. However, evidence specifically linking ROS-induced damage to bone formation as a part of the aging process is quite sparse and the function of aged osteoblasts in molecular cell biology has not been well characterized.

We previously studied the effects of ROS on bone nodule forming activity using cells from the osteoblastic cell line MC3T3-E1 and found that bone nodule formation was significantly reduced by H_2O_2 -treatment[8)]. However, the regulatory mechanisms leading to that observation could not be elucidated, as it is necessary to use a molecular biological approach to comprehensively study the effects of ROS on bone forming activity by osteoblasts. Recently, subtractive gene cloning, a polymerase chain reaction (PCR)-based DNA subtraction method, has been shown to have a number of advantages for cloning

Corresponding author: Yoshimitsu Abiko,2-870-1, sakaecho-nishi, Matsudo, Chiba, Japan, 271-8587.TEL : +81-47-360-9328 FAX: +81-47-360-9329,

differentially expressed genes. This method has been utilized to identify novel genes and may be useful in studies of the mechanisms involved with the decline of bone formation with aging.

In the present study, we used subtractive gene cloning to analysis genes in MC3T3-E1 cells whose expression was altered by H_2O_2. Herein, we describe our subtractive gene cloning strategy and focus on identification of the fibronectin gene, and also show results confirming the effects of H_2O_2 on mRNA expression using a reverse transcription-polymerase chain reaction (RT-PCR) methods.

Materials and Methods

Cell culture and H_2O_2 treatment

MC3T3-E1 cells were purchased from Riken Cell Bank (Ibaraki, Japan). They were seeded at 1×10^5 cells/well in a 24-well culture plate (Corning, Grand Island, NY, USA) and incubated for 24 hours in α-MEM medium containing 5 mM of HEPES supplemented with 50 μg/ml of gentamycin sulfate (Sigma, St. Louis, MO, USA), to which was added 0.3 μg/ml of amphotericin B (Flow Laboratories, VA, USA), 100 units/ml of penicillin G potassium (Sigma, St. Louis, MO, USA), and 10% fetal bovine serum in a humidified atmosphere containing 95% air and 5% CO_2 at 37°C. For RNA isolation, 100-mm diameter dishes were used. The cells were treated with 400 μM of H_2O_2 for 3 hours, after which they were washed and incubated with the differentiation medium, α-MEM medium described above supplemented with 50 μg/ml ascorbic acid and 10 mM β-glycerol phosphate.

Quantitation of bone-nodule formation

For quantitation of bone nodule formation, MC3T3-E1 cells were cultured for 40 and 50 days in the medium, after which the contents of each well were fixed for 15 minutes in 10% neutral buffered formalin and stained using a von Kossa technique.

RNA preparation and construction of subtractive cDNA library

Total cellular RNA was isolated from MC3T3-E1 cells at 6 hours after treatment with or without H_2O_2 using an Rneasy Fibrous Tissue Mini Kit (Qiagen, GmbH, Hilden, Germany) according to the manufacturer's instructions. The cDNA was synthesized by an Omniscript Reverse Transcription kit (Qiagen) according to the manufacture's instructions and utilized a PCR-Select cDNA Subtraction Kit (Clontech) for construction of the subtractive cDNA library, according to the manufacturers' protocols. The resulting cDNA was directly inserted into a pGEM-T Easy Vector (Promega, Madison, WI) and transformed into competent *Escherichia coli* JM109 cells.

Dot-blot differential screening

The cloned cDNA inserts were initially evaluated for differential expression using DNA dot-blot analysis. White colonies from a subtractive cDNA library were picked randomly and the inserts amplified by PCR using the universal vector primers M13 and M13R. The PCR products were then purified with a QIAquick PCR purification kit (Qiagen) and dot-blotted on Hybond-N+ nylon membranes (Amersham Pharmacia Biotech, Buckinghamshire, United Kingdom), after which the membranes were hybridized with horseradish peroxidase (HRP)-labeled tester cDNA as a positive probe and HRP-labeled driver cDNA as a negative probe.

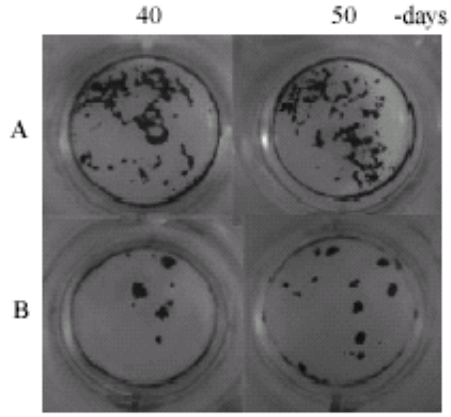

Fig. 1. Effects of H_2O_2 on bone nodule formation by MC3T3-E1 cells. (A) Untreated MC3T3-E1 cells (control). (B) H_2O_2-treated MC3T3-E1 cells.

Nucleotide sequencing and homology search

Sequencing of the cDNA inserts in the vectors was performed using a Big Dye Terminator Cycle Sequencing Kit with T7 primer with an ABI PRIZM 310 Genetic Analyzer (Applied Biosystems, USA). The DNA sequence was analyzed using DNASIS sequence analysis software (Hitachi Software Engineering, Yokohama, Japan). Database homology searches for the cDNA sequence and deduced protein sequences were performed using BLASTN programs with the DNA and protein databases at the National Center for Biotechnology Information (NCBI).

Endpoint RT-PCR and real-time PCR

For the endpoint RT-PCR, PCR amplification was performed on QuantiTect SYBR Green PCR Kit (Qiagen) as instructed by the manufacturer under the following conditions: initial denaturation step of 95°C for 15 mins followed by 20cycles 94°C for 15 sec, 56°C for 30 sec and 72°C for 30 sec. DNA products by endpoint RT-PCR were electrophoresed with DNA size standards on 1.5% agarose gel, followed by staining with ethidium bromide and confirmed the expected size of DNA.

PCR DNA primers used were as follows; 5'-GCGACTCTGACTGGCCTTAC-3' and 5'-C C G T G T A A G G G TCAAAGCAT-3' (Gene bank accession no. NM010233) for FN, 5'-ATCACCATCTTCCAGGAG-3' and 5'-A T G G A C T G

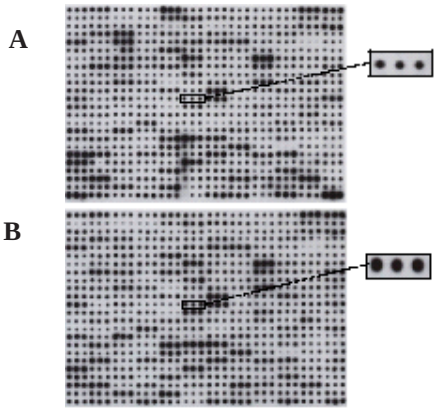

Fig. 2. Dot blot analysis of differentially expressed gene clones. Subtracted DNA samples were dotted onto nylon filters and hybridized with a cDNA probe from H_2O_2-treated or untreated cells.
(A) DNA probe from H_2O_2-treated MC3T3-E1 cells. (B) DNA probe from untreated MC3T3-E1 cells.

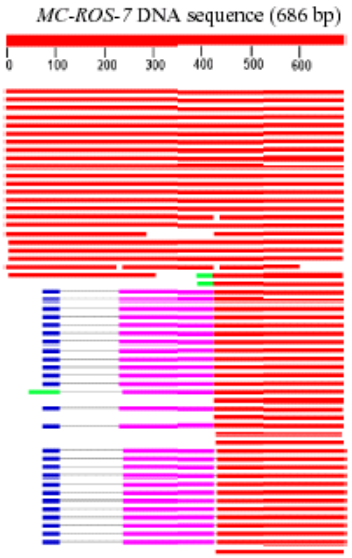

Fig. 3. Homology search for MC-ROS-7 DNA.
(A) Distribution of BLASTN hits in the query sequence.
(B) Identification of a mouse FN gene with homology to MC-ROS-7 DNA.

T G GTCATGAG-3' (Gene bank accession no. M33197) for glyceraldehydes-3-phosphate dehydrogenase (GAPDH). The FN primers were amplified as a product of 166 base pair (bp), the GAPDH primers were amplified as a product of 318 bp.

The real-time PCR was carried out using a QuantiTect SYBR Green PCR Kit (Qiagen). The PCR mixture, which contained 20 pmol of forward and reverse primers and 2 µl of cDNA, was subjected to amplification with a DNA Engine Opticon 1 (MJ Research, San Francisco, CA, USA). The cycles were set at 95°C for 15 min for preheating, followed by 36 cycles at 94°C for 15 sec, 56°C for 30 sec and 72°C for 30 sec. The amplicons were detected directly by measuring the increase in fluorescence caused by the binding of the SYBR Green I dye to gene-specific, amplified, double-stranded DNA using a DNA Engine Opticon 1. Following the completion of the PCR reaction, the temperature was raised from the annealing temperature to 95°C for a melting curve analysis.

Table 1

Gene ID	Description	Identity (%)
NM_010233	Mus musculus fibronectin 1 (Fn1), mRNA.	99.7
AK147315	Mus musculus cDNA, fibronectin 1	99.7
AK147249	Mus musculus cDNA, fibronectin 1	99.7
AK133868	Mus musculus 8 days embryo, fibronectin 1	99.7
AK147701	Mus musculus 14 days female placenta, fibronectin 1	99.7
AK147683	Mus musculus 14 days female placenta, fibronectin 1	99.6
AK147663	Mus musculus 14 days female placenta, fibronectin 1	99.6
AK147639	Mus musculus 14 days female placenta, fibronectin 1	99.6
AK159794	Mus musculus osteoclast-like cell cDNA•Afibronectin 1	99.6
AK170755	Mus musculus dendritic cells, fibronectin 1	99.6
BC025521	Mus musculus fibronectin 1, mRNA	99.6
BC036167	Mus musculus fibronectin 1, mRNA	99.6
BC004724	Mus musculus fibronectin 1, mRNA	99.6
AK090130	Mus musculus bone marrow stroma cell, fibronectin 1	99.4
AK090135	Mus musculus bone marrow stroma cell, fibronectin 1	99.3
M18194	Mouse fibronectin (FN) mRNA.	98.1
NM_019143	Rattus norvegicus fibronectin 1 (Fn1), mRNA	92.9
X15906	Rat mRNA for fibronectin	92.9
L29191	Rat fibronectin	92.7

NM-010233.1: Mus musculus fibronectin 1 (Fn1), mRNA Identities =684/686 (99.7%)

```
Query  1     ACTGAAACCCTGAAGCAGAACAGGGTGACCAACTGTCACCATTGAGGAGAGAAGTCTCAA  60
Sbjct  7859  ACTGAAACCCTGAAGCAGAACAGGGTGACCAACTGTCACCATTGAGGAGAGAAGTCTCAA  7800

Query  61    AACATCCCACGGGGCGATGCTTGGAGAAGCTGTAAATTGTGCTGAAGCTGAGAACATGGC  120
Sbjct  7799  AACATCCCACGGGGCGATGCTTGGAGAAGCTGTAAATTGTGCTGAAGCTGAGAACATGGC  7740

Query  121   TCCAGGGCAAAAGGCTTAAGGGTGAAAGGACCACTCAAAGATGGAGGGTCTGCTAACATC  180
Sbjct  7739  TCCAGAGCAAAAGGCTTAAGGGTGAAAGGACCACTCAAAGATGGAGGGTCTGCTAACATC  7680

Query  181   ACTGGGGTGTGGATTGACCTTGGTAGAGAGACACTTGTAGGGTGGGGCTGGAAAGATTAC  240
Sbjct  7679  ACTGGGGTGTGGATTGACCTTGGTAGAGAGACACTTGTAGGGTGGGGCTGGAAAGATTAC  7620

Query  241   TCTCGAGAATCGTCTCTGTCAGCTTGCACATCTAGCGGCATGAAGCACTCAATGGGGCAA  300
Sbjct  7619  TCTCGAGAATCGTCTCTGTCAGCTTGCACATCTAGCGGCATGAAGCACTCAATGGGGCAA  7560

Query  301   TTTACGTTAGTGTTTGTTCTCTGATTGTATCTCTGTGTATACTGGTTGTAGGTGTGGCCG  360
Sbjct  7559  TTTACGTTAGTGTTTGTTCTCTGATTGTATCTCTGTGTATACTGGTTGTAGGTGTGGCCG  7500

Query  361   GTGGTGCCATCGGGACTGGGTTCAGCAGCCCCAGGTCTACGGCAGTTGTCACAGCGCCAG  420
Sbjct  7499  GTGGTGCCATCGGGACTGGGTTCAGCAGCCCCAGGTCTACGGCAGTTGTCACAGCGCCAG  7440

Query  421   CC  422
              ||
Sbjct  7439  CC  7438

Query  423   GGGGATCACACTTGAATTCTCCCTTTCCATTCCCGAGGCATGTGCAGCTCATCCGCTGGC  482
Sbjct  7330  GGGGATCACACTTGAATTCTCCCTTTCCATTCCCGAGGCATGTGCAGCTCATCCGCTGGC  7271

Query  483   CATTTTCTCCCTGCCGATCCCACTTCTCTCCGATCTTGTAGTTGACACCGTTGTCATGGC  542
Sbjct  7270  CATTTTCTCCCTGCCGATCCCACTTCTCTCCGATCTTGTAGTTGACACCGTTGTCATGGC  7211

Query  543   ACCATTTAGATGAATCGCATCTGAAATGACC-CTGCCAAAGCCCAAGCACTGGCATTGTG  601
Sbjct  7210  AGCATTTAGATGAATGGCATGTGAAATGAGCAGTGGCAAAGGGCAAGCAGTGGCA-TGTG  7152

Query  602   AGCTTAAAGCCAGCGTCAGACAACCGCTCCCACTCCT-TCCAATGGCGTAATGGGAAACC  660
Sbjct  7151  AGCTTAAAGCCAGCGTCAGACAACCGCTCCCACTCCTCTCCAATGGCGTAATGGGAAACC  7092

Query  661   GTGTAAGGGTCAAAGCATGAGTCATC  686
              |||||||||||||||||||||||||
Sbjct  7091  GTGTAAGGGTCAAAGCATGAGTCATC  7066
```

Fig

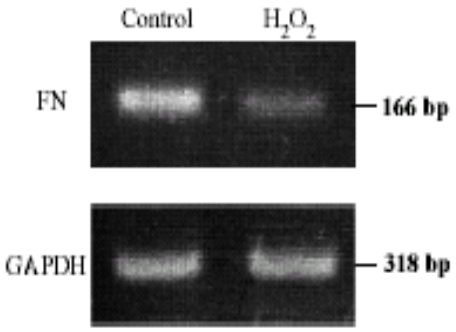

Figure 4. Endpoint RT-PCR analysis of FN mRNA levels.
An ethidium bromide staining pattern of the amplified PCR products using agarose gel electrophoresis is shown. FN mRNA was expressed at a lower level in the H_2O_2-treated MC3T3-E1 cells as compared to untreated cells.

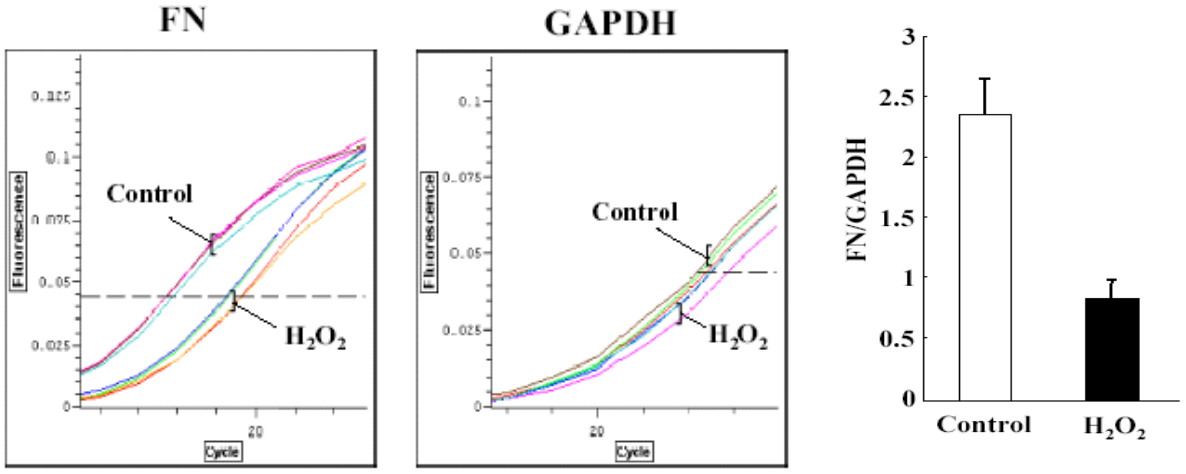

Figure 5. Real-time PCR detection of FN mRNA levels.
(A) Exponential curves of fluorescence intensity detected during the PCR cycle are shown on the vertical axis of a logarithmic scale (n=3). (B) Expression of the FN gene determined by real-time PCR data, which are shown as normalized values divided by the results for GAPDH (FN/GAPDH). Significant decreases (*p•ƒ0.05, n=3) in FN gene expression levels in H_2O_2-treated MC3T3-E1 cells were observed.

Results

As shown in Figure 1, bone nodule formation was significantly reduced in MC3T3-E1 cells following treatment with H_2O_2 as compared with the untreated cells. Next, we isolated RNA from both H_2O_2-treated and untreated cells, and examined differential gene expression by the subtractive gene cloning.

A triple dot-blot analysis of subtracted DNA to screen the expressed genes is shown in Figure 2. Several of the subtracted gene clones were differentially expressed in the initial tester and driver samples. Among those, a gene clone designated as MC-ROS -7, which showed an intensity of 3 dots, was significantly reduced in H_2O_2-treated cells as compared to the control cells.

Next, nucleotide sequencing of MC-ROS-7 and a homology search were carried out. The BLASTN search resulted in a number of BLAST hits in the query sequence with a variety of homologies. Figure 3A shows the distribution of BLASTN search hits in the query sequence. Among the genes found, MC-ROS-7 DNA exhibited a 99.7% homology to the Mus musculus fibronectin 1 (FN) gene (Figure 3B). Genes with high homology sequences with MC-ROS-7 in the DNA database are summarized in Table 1. To confirm the reduced mRNA level in the FN gene from H_2O_2-treated cells, endpoint RT-PCR analysis was performed. A significantly lower level of FN mRNA was found in H_2O_2-treated cells as compared to untreated cells, while the mRNA levels of GAPDH, used as a housekeeping control gene, were the same with or without H_2O_2-treatment (Fig. 4).

Additional experiments to determine the precise rates of enhancement of the FN genes were performed using real-time PCR. PCR exponential curves of the FN and GAPDH genes are shown in Figure 5A, with data obtained following conversion to relative mRNA amounts and the ratio of FN/GAPDH calculated for standardization shown in Figure 5B. A significant reduction of FN gene expression was observed in H_2O_2-treated cells.

Discussion

The extracellular matrix (ECM) is known to act as a substratum in a variety of tissues and plays an important role in cellular functions. FN is a heterodimeric ECM glycoprotein that has been shown to regulate the adhesion, migration, and differentiation of various mesenchymal cells[9]. Interestingly, FN deposition on the cell surface has been reported to be decreased in human aged fibroblasts[10], while FN isolated from late passage fibroblasts has been described as unable to support normal cell substrate interactions[11].

Previously, we investigated hydroxy radicals generated by H_2O_2-Cu ion on degraded and/or modified FN proteins. Bone nodule formation by rat osteoblasts in FN-coated culture dishes was significantly greater than in the non-coated dishes, while that in FN-coated dishes following hydroxy radicals treatment was significantly less than without such treatment[12]. Further, alkaline phosphatase activity in and the secretion of type I collagen from those osteoblasts were reduced by FN-treated hydroxy radicals. RT-PCR analysis also showed that mRNA levels of alkaline phosphatase and type I collagen genes were diminished by treatment with hydroxy radicals[13]. Thus, tissue aging may be directly related to altered interactions between cells and the ECM. However, the direct effect of ROS on the gene expression of FN in osteoblasts is not well documented.

In the present study, we attempted to identify the effects of H_2O_2 on gene expression in MC3T3-E1 cells using subtractive gene cloning technology. Based on our results, we selected MC-ROS-7 cells, which showed reduced mRNA expression following H_2O_2 treatment. To confirm the gene product of MC-ROS-7, we used nucleotide sequencing of MC-ROS-7 DNA and conducted a homology search of the NCBI BLAST nucleic acid databases. We found that the DNA sequence of MC-ROS-7 exhibited a high homology to that of FN. We also analyzed mRNA levels in H_2O_2

-treated and untreated MC3T3-E1 cells using endpoint PCR and real-time PCR assays. As expected, a significant lower level of FN mRNA was observed in the H_2O_2-treated cells as compared to that in untreated cells. These findings suggest that transcription of the FN gene in MC3T3-E1 cells is reduced following challenge with ROS.

Based on our results, we concluded that ROS may cause a decline in bone formation through a reduction of FN gene expression and a disfunction of the FN protein by degradation and/or modification during the ageing process.

Acknowledgement

This work was supported by "Academic Frontier" Project for Private Universities: matching fund subsidy from Ministry of Education, Culture, Sports, Science and Technology, and by Grant-in-Aid for Scientific Research (A1-16209063) from Japan Society for the Promotion of Science.

References

1) Rodan G.A.: Introduction to bone biology. Bone, Supp l: S3-S6, 1992.
2) Roholl P.J., Blauw E., Zurcher C., Dormans J.A. and Theuns H.M.: Evidence for a diminished maturation of preosteoblasts into osteoblasts during aging in rats: an ultrastructural analysis. J Bone Miner Res, 9: 355-366, 1994.
3) Golden T.R., Hinerfeld D.A. and Melov. S.: Oxidative stress and aging: beyond correlation. Aging Cell, 1:117-123, 2002.
4) Finkel T. and Holbrook N.J.: Oxidants, oxidative stress and the biology of ageing. Nature, 408: 239-247, 2000.
5) Maggio D., Barabani M., Pierandrei M., Polidori M.C., Catani M., Mecocci P., Senin U., Pacifici R. and Cherubini A.: Marked decrease in plasma antioxidants in aged osteoporotic women: results of a cross-sectional study. J Clin Endocrinol Metab, 88: 1523-1527, 2003.
6) Tyner S.D., Venkatachalam S., Choi J., Jones S., Ghebranious N., Igelmann H., Lu X., Soron G., Cooper B., Brayton C., Hee Park S., Thompson T., Karsenty G., Bradley A. and Donehower L.A.: p53 mutant mice that display early ageing-associated phenotypes. Nature, 415: 45-53, 2002.
7) de Boer J., Andressoo J.O., de Wit J., Huijmans J., Beems R.B., van Steeg H., Weeda G., van der Horst G.T., van Leeuwen W., Themmen A.P., Meradji M. and Hoeijmakers J.H. : Premature aging in mice deficient in DNA repair and transcription. Science, 296: 1276-1279, 2002.
8) Otsuka-Tanaka Y., Sato T., Fujita T., Suzuki H., Kawara M., Abiko Y. and Mega J.: Reduction of bone nodule formation in MC3T3-E1 cells by treatment with hydrogen peroxide. Int J Orasl-Med Sci, in press.
9) Yamada, K., Aota, S., Akiyama, A. and LaFlamme, S.: Mechanisms of fibronectin and integrin function during cell adhesion and migration. Cold Spring Harbor Symp. Quant. Biol LVII, 1992, pp 203-212.
10) Aizawa S., Mitsui Y., Kurimoto F. and Nomura K.: Cell surface changes accompanying aging in human diploid fibroblast. Exp Cell Res, 127:143-157, 1980.
11) Chandrasekhar S., Sorrentino J.A. and Millis A.J.T.: Interaction of fibronectin with collagen: Age-specific defect in the biological activity of human fibroblast fibronectin. Proc Natl Acad Sci, 80: 4747-4751, 1983.
12) Suzuki, H., Hayakawa, M., Kobayashi, K. and Abiko, Y.: H_2O_2-derived free radical-treated fibronectin substratum reduces bone nodule formation of rat calvarial osteoblasts. Mech Aging Dev, 98:113-125, 1997.
13) Hosoya, S., Suzuki, H., Yamamoto, M., Kobayashi, K. and Abiko, Y.: Alkaline phosphatase and type É collagen gene expression were reduced by hydroxyl radical-treated fibronectin substratum. Mol Genet Metab, 65:31-34, 1998.